

DYSON SCHWINGER EQUATIONS:
CONNECTING SMALL AND LARGE LENGTH-SCALES

CRAIG ROBERTS

Physics Division, 203, Argonne National Laboratory, Argonne IL 60439, USA

I illustrate the phenomenological application of Dyson-Schwinger equations to the calculation of meson properties observable at TJNAF. Particular emphasis is given to this framework's ability to unify long-range effects constrained by chiral symmetry with short-range effects prescribed by perturbation theory, and interpolate between them.

PACS numbers: 12.38.Lg, 13.40.Gp, 14.40.Aq, 24.85.+p

Keywords: Dyson-Schwinger Equations, Nonperturbative methods, Continuum QCD, Confinement, Dynamical chiral symmetry breaking, Pion electromagnetic and anomalous transition form factors

1. Dressed Quarks

The Dyson-Schwinger equations (DSEs) [1] provide a nonperturbative approach to studying the continuum formulation of QCD, making accessible phenomena such as confinement, dynamical chiral symmetry breaking (DCSB) and bound state structure. However, they also provide a generating tool for perturbation theory and hence their phenomenological application is tightly constrained at high-energy. This is the particular feature of the phenomenological application of DSEs: their ability to furnish a unified description of high- and low-energy phenomena in QCD. It is elucidated in Refs. 2,3 and here I only illustrate this aspect, using as primary exemplars the electromagnetic pion form factor and the $\gamma^*\pi \rightarrow \gamma$ transition form factor, which are particularly relevant to the TJNAF community.

A key element in the description of hadronic observables is the dressing of the quark propagator, which is described by the quark DSE:

$$\begin{aligned} S_f(p)^{-1} &:= i\gamma \cdot p A_f(p^2) + B_f(p^2) = A_f(p^2) (i\gamma \cdot p + M_f(p^2)) & (1) \\ &= Z_2(i\gamma \cdot p + m_f^{\text{bm}}) + Z_1 \int_q^\Lambda g^2 D_{\mu\nu}(p-q) \frac{\lambda^a}{2} \gamma_\mu S_f(q) \Gamma_\nu^{fa}(q,p). & (2) \end{aligned}$$

Here f is a flavour label, $D_{\mu\nu}(k)$ is the dressed-gluon propagator [4,5], $\Gamma_\nu^{fa}(q,p)$ is the dressed-quark-gluon vertex, m_f^{bm} is the Λ -dependent current-quark bare mass and $\int_q^\Lambda := \int^\Lambda d^4q/(2\pi)^4$ represents mnemonically a *translationally-invariant* regularisation of the integral, with Λ the regularisation mass-scale. The quark-gluon-vertex and quark wave function renormalisation constants, Z_1 and Z_2 , depend on the renormalisation point, ζ , and the regularisation mass-scale.

The qualitative features of the solution of Eq. (2) are known. In QCD the chiral limit is defined by $\hat{m} = 0$, where \hat{m} is the renormalisation-point-independent current-quark mass. For $\hat{m} = 0$ there is no mass-like divergence in the perturbative

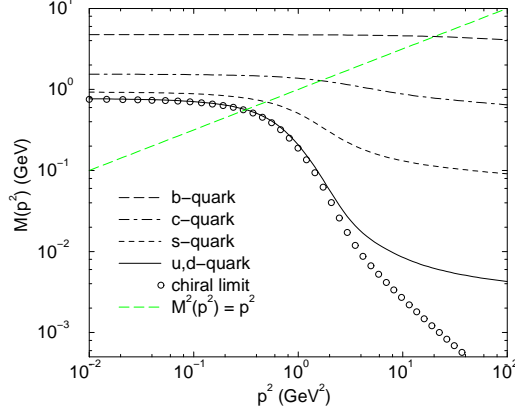


Figure 1: Quark mass function obtained as a solution of Eq. (2) using $D_{\mu\nu}(k)$ and $\Gamma_{\nu}^{fa}(q, p)$ from Ref. 6, and $m_{u,d}^{\zeta} = 3.7 \text{ MeV}$, $m_s^{\zeta} = 82 \text{ MeV}$, $m_c^{\zeta} = 0.58 \text{ GeV}$ and $m_b^{\zeta} = 3.8 \text{ GeV}$ ($\zeta = 19 \text{ GeV}$). The indicated solutions of $M^2(p^2) = p^2$ define the Euclidean constituent-quark mass, M_f^E , which takes the values: $M_{u,d}^E = 0.56 \text{ GeV}$, $M_s^E = 0.70 \text{ GeV}$, $M_c^E = 1.3 \text{ GeV}$, $M_b^E = 4.6 \text{ GeV}$.

evaluation of the quark self energy and hence for $p^2 > 20 \text{ GeV}^2$ the solution of Eq. (2) is [6]

$$M_0(p^2) \stackrel{\text{large-}p^2}{=} \frac{2\pi^2\gamma_m}{3} \frac{(-\langle\bar{q}q\rangle^0)}{p^2 \left(\frac{1}{2} \ln [p^2/\Lambda_{\text{QCD}}^2]\right)^{1-\gamma_m}}, \quad (3)$$

where $\gamma_m = 12/(33 - 2N_f)$ is the gauge-independent mass anomalous dimension and $\langle\bar{q}q\rangle^0$ is the renormalisation-point-independent vacuum quark condensate. The momentum-dependence is a model-independent result. The existence of DCSB means that $\langle\bar{q}q\rangle^0 \neq 0$, however, its actual value depends on the long-range behaviour of $D_{\mu\nu}(k)$ and $\Gamma_{\nu}^{0a}(q, p)$, which is modelled in contemporary DSE studies. Requiring a good description of light-meson observables necessitates $\langle\bar{q}q\rangle^0 \approx -(0.24 \text{ GeV})^3$.

In contrast, for $\hat{m}_f \neq 0$,

$$M_f(p^2) \stackrel{\text{large-}p^2}{=} \frac{\hat{m}_f}{\left(\frac{1}{2} \ln [p^2/\Lambda_{\text{QCD}}^2]\right)^{\gamma_m}}. \quad (4)$$

An obvious qualitative difference is that, relative to Eq. (4), the chiral-limit solution is $1/p^2$ -suppressed in the ultraviolet.

There is some quantitative model-dependence in the p^2 -evolution of $M_f(p^2)$ into the infrared. However, for any forms of $D_{\mu\nu}$ and Γ_{ν}^{fa} that provide an accurate description of $f_{\pi,K}$ and $m_{\pi,K}$, one obtains profiles like those illustrated in Fig. 1.

The evolution to coincidence between the chiral-limit and u, d -quark mass functions, apparent in this figure, makes clear the transition from the perturbative to the nonperturbative domain. The chiral limit mass-function is nonzero *only* because of the nonperturbative DCSB mechanism whereas the u, d -quark mass function is purely perturbative at $p^2 > 20 \text{ GeV}^2$, where Eq. (4) is accurate. The DCSB mechanism thus has a significant effect on the propagation characteristics of u, d, s -quarks, and this is fundamentally important in QCD with observable consequences.

2. Bound States

A meson is a bound state of a dressed-quark and -antiquark, and its internal structure is described by a Bethe-Salpeter amplitude obtained as the solution of

$$[\Gamma_P(k; Q)]_{tu} = \int_q^\Lambda [\chi_P(q; Q)]_{sr} K_{tu}^{rs}(q, k; Q), \quad (5)$$

where $\chi_P(q; Q) = \mathcal{S}(q_+) \Gamma_P(q; Q) \mathcal{S}(q_-)$; $\mathcal{S}(q) = \text{diag}(S_u(q), S_d(q), S_s(q), \dots)$; $q_+ = q + \eta_Q Q$, $q_- = q - (1 - \eta_Q) Q$, with Q the total momentum of the bound state and $\eta_Q \in [0, 1]$ the relative-momentum partitioning parameter; and r, \dots, u represent colour-, Dirac- and flavour-matrix indices. For a pseudoscalar meson, such as the pion, the solution has the general form

$$\begin{aligned} \Gamma_P(k; Q) = T^P \gamma_5 & \left[iE_P(k; Q) + \gamma \cdot Q F_P(k; Q) \right. \\ & \left. + \gamma \cdot k k \cdot Q G_P(k; Q) + \sigma_{\mu\nu} k_\mu Q_\nu H_P(k; Q) \right], \end{aligned} \quad (6)$$

where T^P is a flavour matrix identifying the meson; e.g., $T^{\pi^+} = \frac{1}{2} (\lambda^1 + i\lambda^2)$, with $\{\lambda^j, j = 1 \dots N_f^2 - 1\}$ the Gell-Mann matrices of $SU(N_f)$.

In Eq. (5), K is the renormalised, fully-amputated, quark-antiquark scattering kernel. Important in the successful application of DSEs is that K has a systematic skeleton expansion in terms of the elementary dressed-particle Schwinger functions; e.g., the dressed-quark and -gluon propagators. The expansion introduced in Ref. 7 provides a means of constructing a kernel that, order-by-order in the number of vertices, ensures the preservation of vector and axial-vector Ward-Takahashi identities; i.e., current conservation. Only with such a truncation is an accurate description of the light-quark mesons possible.

In QCD the leptonic decay constant of a pseudoscalar meson is [6]

$$f_P Q_\mu = \text{tr} Z_2 \int_k^\Lambda (T^P)^T \gamma_5 \gamma_\mu \chi_P(k; Q), \quad (7)$$

where the trace is over colour, Dirac and flavour indices. Equation (7) is *exact*: the Λ -dependence of Z_2 ensures that the right-hand-side (r.h.s.) is finite as $\Lambda \rightarrow \infty$, and its ζ - and gauge-dependence is just that necessary to compensate that of $\chi_P(k; Q)$.

In the chiral limit the axial-vector current is conserved, and employing any Ward-Takahashi identity preserving truncation of K one obtains

$$\begin{aligned} f_P E_P(k; 0) &= B_0(k^2), & F_R(k; 0) + 2 f_P F_P(k; 0) &= A_0(k^2), \\ G_R(k; 0) + 2 f_P G_P(k; 0) &= 2A'_0(k^2), & H_R(k; 0) + 2 f_P H_P(k; 0) &= 0, \end{aligned} \quad (8)$$

where F_R , G_R and H_R are calculable functions in the dressed axial-vector vertex, $\Gamma_{5\mu}^H(k; Q)$. These identities are associated with Goldstone's theorem and in fact one can show [6] that when chiral symmetry is dynamically broken: 1) the flavour-nonsinglet, pseudoscalar BSE has a massless solution; 2) the Bethe-Salpeter amplitude for the massless bound state has a term proportional to γ_5 alone, with the momentum-dependence of $E_P(k; 0)$ completely determined by that of $B_0(k^2)$, in addition to terms proportional to other pseudoscalar Dirac structures that are nonzero; and 3) $\Gamma_{5\mu}^P(k; Q)$ is dominated by the pseudoscalar bound state pole for $Q^2 \simeq 0$. The converse is also true. Hence, in the chiral limit, the pion is a massless composite of a quark and an antiquark, each of which has an effective mass $M^E \sim 0.5 \text{ GeV}$.

For nonzero values of the current-quark mass, whether small or large, instead of Eqs. (8) one obtains [6]

$$f_P^2 m_P^2 = -\mathcal{M}_P \langle \bar{q}q \rangle_\zeta^P, \quad (9)$$

where $\mathcal{M}_P = \text{tr}_f \left[M_{(\zeta)} \left\{ T^P, (T^P)^T \right\} \right]$ e.g., for the π : $\mathcal{M}_{\pi^+} = m_u^\zeta + m_d^\zeta$, and

$$-\langle \bar{q}q \rangle_\zeta^P = f_P \text{tr} Z_4 \int_q^\Lambda (T^P)^T \gamma_5 \chi_P(q; Q). \quad (10)$$

Equation (9) is an exact mass formula for flavour non-singlet mesons and I note that the r.h.s. does not involve a difference of massive quark propagators: a phenomenological assumption often employed. $\langle \bar{q}q \rangle_\zeta^P$ in Eq. (10) is an ‘‘in-hadron’’ condensate. It is gauge-independent and its renormalisation point dependence is exactly that required to ensure that the r.h.s. of Eq. (9) is renormalisation point *independent*.

For small current-quark masses, $\hat{m}_q \sim 0$, Eq. (9) yields what is commonly called the Gell-Mann–Oakes–Renner relation; i.e., $m_P^2 \propto \hat{m}_q$, because

$$\lim_{\hat{m} \rightarrow 0} \langle \bar{q}q \rangle_\zeta^P = \langle \bar{q}q \rangle_\zeta^0. \quad (11)$$

However, it also has an important corollary when the current-mass, \hat{m}_Q , of one or both constituents becomes large, predicting [8]

$$m_P \propto \hat{m}_Q, \quad (12)$$

which follows because $\langle \bar{q}q \rangle_\zeta^P$ is \hat{m}_Q -independent for large- \hat{m}_Q and $f_P \propto m_P^{-1/2}$. The transition from the quadratic to the linear mass-relation occurs at $\hat{m}_q \approx 2 \hat{m}_s$ [9], at which point explicit chiral symmetry breaking overwhelms DCSB.

Two other important model-independent results can be obtained [6] from Eq. (5) and the systematic construction of K . The scalar functions in Eq. (6) depend on three invariants; e.g., $E_P(k; Q) = E_P(k^2, k \cdot Q, Q^2)$. The zeroth Chebyshev moment of these functions; e.g.,

$${}^0E_P(k^2, Q^2) := \frac{2}{\pi} \int_0^\pi dx \sqrt{1-x^2} E_P(k; Q), \quad k \cdot Q := x \sqrt{k^2 Q^2} \quad (13)$$

are dominant in the description of bound state properties, and

$${}^0E_P(k^2, Q^2) \stackrel{\text{large-}k^2}{\propto} M_0(k^2), \quad (14)$$

with ${}^0F_P(k^2, Q^2)$, $k^2 {}^0G_P(k^2, Q^2)$ and $k^2 {}^0H_P(k^2, Q^2)$ behaving in precisely the same way. Further

$$k^2 {}^0G_P(k^2, Q^2) \stackrel{\text{large-}k^2}{\propto} 2 {}^0F_P(k^2, Q^2). \quad (15)$$

These results determine the asymptotic form of the electromagnetic pion form factor.

3. Electromagnetic Pion Form Factor

The impulse approximation to the electromagnetic pion form factor is [10]

$$(p_1 + p_2)_\mu F_\pi(q^2) := \Lambda_\mu(p_1, p_2) \quad (16)$$

$$= 2N_c \text{tr}_D \int_k^\Lambda \bar{\Gamma}_\pi(k; -p_2) S(k_{++}) i\Gamma_\mu^\gamma(k_{++}, k_{+-}) S(k_{+-}) \Gamma_\pi(k_{0-}; p_1) S(k_{--}),$$

where $\bar{\Gamma}_\pi(q; -P)^\text{T} := C^{-1} \Gamma_\pi(-q; -P) C$ with $C = \gamma_2 \gamma_4$, the charge conjugation matrix, and $k_{\alpha\beta} := k + \alpha p_1/2 + \beta q/2$, $p_2 := p_1 + q$. No renormalisation constants appear explicitly in Eq. (16) because the renormalised dressed-quark-photon vertex, Γ_μ^γ , satisfies the vector Ward-Takahashi identity. This also ensures current conservation: $(p_1 - p_2)_\mu \Lambda_\mu(p_1, p_2) = 0$.

The calculation of $F_\pi(q^2)$ is simplified by using a model algebraic parametrisation of the dressed-quark propagator that efficiently characterises the essential elements of the solution of the quark-DSE and determines the pion Bethe-Salpeter amplitude via Eqs. (8) and (15), and an efficacious *Ansatz* [11] for Γ_μ^γ in which the vertex is completely determined by the dressed-quark propagator. The result is depicted in Fig. 2. The current uncertainty in the experimental data at intermediate q^2 is apparent in the lower panel, as is the difference between the results calculated with or without the pseudovector components: F , G , of the pion Bethe-Salpeter amplitude. These components provide the dominant contribution to $F_\pi(q^2)$ at large pion energy [10] because of the multiplicative factors: $\gamma \cdot Q$ and $\gamma \cdot k k \cdot Q$, which contribute an additional power of q^2 in the numerator of those terms involving F^2 , FG and G^2 relative to those proportional to E . Including them one finds

$$F_\pi(q^2) \stackrel{\text{large-}q^2}{\propto} \frac{\alpha(q^2)}{q^2} \frac{(-\langle \bar{q}q \rangle_{q^2}^0)^2}{f_\pi^4}; \quad (17)$$

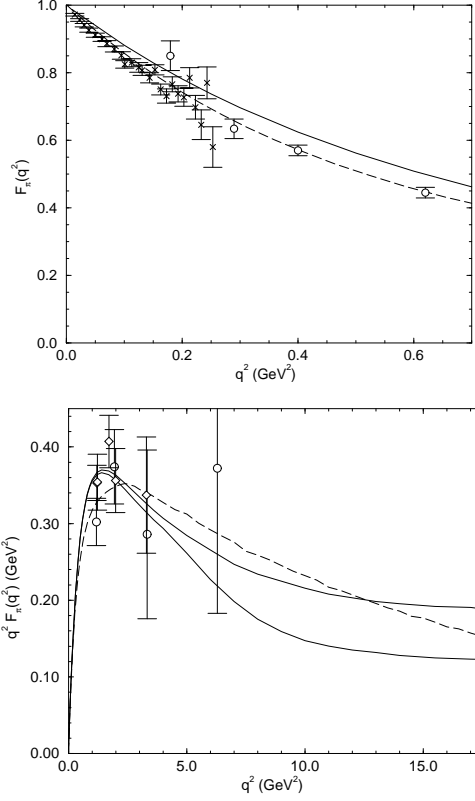


Figure 2: Upper panel: calculated pion form factor compared with data at small- q^2 . Lower panel: the large- q^2 comparison, with the two solid lines showing the range of model-dependent uncertainty. In both panels the dashed line [13] assumes that $F_\pi = 0 = G_\pi = H_\pi$, and the data are taken from Refs. 12.

i.e., $q^2 F_\pi(q^2) \approx \text{const.}$, up to calculable $\ln q^2$ -corrections, in agreement with the expectations raised by perturbative QCD. If the pseudovector components of Γ_π are neglected, the additional numerator factor of q^2 is missing and one obtains [13] $q^4 F_\pi(q^2) \approx \text{const.}$.

4. $\gamma^* \pi \rightarrow \gamma$ Transition Form Factor

The impulse approximation to this form factor is

$$\begin{aligned}
 T_{\mu\nu}^3(k_1, k_2) &:= \frac{1}{4\pi^2} i\varepsilon_{\mu\nu\rho\sigma} k_{1\rho} k_{2\sigma} \hat{T}(k_1^2, k_1 \cdot k_2, k_2^2) \\
 &= \text{tr} \int_q^\Lambda S(q_1) \Gamma_\pi(\hat{q}; -P) S(q_2) i\mathcal{Q}\Gamma_\mu^\gamma(q_2, q_{12}) S(q_{12}) i\mathcal{Q}\Gamma_\nu^\gamma(q_{12}, q_1),
 \end{aligned} \tag{18}$$

where $\mathcal{Q} = (\frac{1}{3}I + \tau^3)/2 = \text{diag}(2/3, -1/3)$, and k_1, k_2 are the photon momenta [on-shell: $k_1^2 = 0 = k_2^2$, $2k_1 \cdot k_2 = P^2$], q is the loop-momentum, and $q_1 := q - k_1$, $q_2 := q + k_2$, $\hat{q} := \frac{1}{2}(q_1 + q_2)$, $q_{12} := q - k_1 + k_2$. The manner in which the ‘‘triangle anomaly’’ is recovered with no dependence on model parameters is described in Ref. [10], and this same mechanism applies to all anomalous pion and photopion processes [14]. It is a unique feature of the DSE framework.

Using this expression one can calculate [15,16] $\hat{T}(k_1^2, k_1 \cdot k_2, k_2^2)$ when one or both of the photons is off shell and also determine the asymptotic behaviour analytically. The formal character of that derivation is presented in Ref. 16 but, in neglecting essential aspects of renormalisation, it is imprecise. I remedy that here for the illustrative case of one photon off-shell: $k_1^2 = Q^2$.

At large- Q^2 , $k_1 \cdot k_2 \approx -Q^2/2$, and in Eq. (18) the pion Bethe-Salpeter amplitude focuses the integration support at $\hat{q} = 0$. As a consequence the asymptotic behaviour of the integral can be determined using

$$S(q_{12}) \approx \frac{1}{Z_2} \frac{1}{Q^2} i\gamma \cdot (k_1 - k_2), \quad \Gamma_\mu^\gamma \approx Z_1 \gamma_\mu, \quad (19)$$

which follow from Eq. (2) and the DSE for the quark-photon vertex, so that

$$T_{\mu\nu}^3(k_1, k_2) \approx i \frac{1}{Q^2} (k_1 - k_2)_\sigma \text{tr} Z_2 \int_q^\Lambda \frac{1}{6} \tau^3 \chi_\pi(\hat{q}; -P) \gamma_\mu \gamma_\sigma \gamma_\nu, \quad (20)$$

where I have used the Ward identity: $Z_1 = Z_2$. Hence, the transition form factor

$$\begin{aligned} \frac{1}{4\pi^2} i\varepsilon_{\mu\nu\rho\sigma} k_{1\rho} k_{2\sigma} T(Q^2) &:= T_{\mu\nu}^3(k_1, k_2) + T_{\nu\mu}^3(k_2, k_1) \\ &\approx -\frac{1}{Q^2} i\varepsilon_{\mu\nu\rho\sigma} (k_1 - k_2)_\rho \frac{2}{3} \text{tr} Z_2 \int_q^\Lambda \frac{1}{2} \tau^3 \chi_\pi(\hat{q}; -P) \gamma_5 \gamma_\sigma \end{aligned} \quad (21)$$

$$= i\varepsilon_{\mu\nu\rho\sigma} k_{1\rho} k_{2\sigma} \frac{4}{3} \frac{f_\pi}{Q^2}, \quad (22)$$

where the last line follows from Eq. (7); i.e.,

$$T(Q^2) \stackrel{\text{large-}Q^2}{\approx} \frac{4}{3} \frac{4\pi^2 f_\pi}{Q^2}, \quad (23)$$

in agreement with the expectations raised by perturbative QCD. Thus, as with Eq. (16), one equation unifies the small- and large- Q^2 results and predicts the evolution between them [15-17].

5. Epilogue

I have been necessarily brief. There are many other applications of interest to this community, among them the diffractive electroproduction of neutral vector

mesons [18], the electromagnetic form factors of their charged states [19] and the unification of light- and heavy-meson observables [8]. The most pressing contemporary challenge relevant to this community is the extension of the framework to the calculation of baryon observables, which is underway.

Acknowledgments

I would like to thank Dubravko Klabucar and the organisers for their assistance, kindness and hospitality. This work was supported by the US Department of Energy, Nuclear Physics Division, under contract number W-31-109-ENG-38, and the National Science Foundation, under grant no. INT-9603385.

References

1. C.D. Roberts and A.G. Williams, Prog. Part. Nucl. Phys. **33** (1994) 477.
2. P.C. Tandy, Prog. Part. Nucl. Phys. **39** (1997) 117.
3. C.D. Roberts, “Nonperturbative QCD with modern tools,” nucl-th/9807026.
4. M.R. Pennington, “Calculating hadronic properties in strong QCD,” hep-ph/9611242.
5. R. Alkofer, S. Ahlig and L.v. Smekal, “The infrared behavior of gluon, ghost, and quark propagators in Landau gauge QCD,” hep-ph/9901322, these proceedings.
6. P. Maris and C.D. Roberts, Phys. Rev. **C56** (1997) 3369.
7. A. Bender, C.D. Roberts and L. v. Smekal, Phys. Lett. **B380** (1996) 7.
8. M.A. Ivanov, Y.L. Kalinovsky and C.D. Roberts, “Survey of heavy-meson observables”, nucl-th/9812063.
9. P. Maris and C.D. Roberts, “Differences between heavy and light quarks,” nucl-th/9710062.
10. P. Maris and C.D. Roberts, Phys. Rev. **C58** (1998) 3659.
11. J.S. Ball and T. Chiu, Phys. Rev. **D22** (1980) 2542.
12. S.R. Amendolia *et al.*, Nucl. Phys. **B277** (1986) 168; C.J. Bebek *et al.*, Phys. Rev. **D13** (1976) 25; C.J. Bebek *et al.*, Phys. Rev. **D17** (1978) 1693.
13. C.D. Roberts, Nucl. Phys. **A605** (1996) 475.
14. C.D. Roberts, R.T. Cahill and J. Praschifka, Ann. Phys. **188** (1988) 20; R. Alkofer and C.D. Roberts, Phys. Lett. **B 369** (1996) 101.
15. M.R. Frank, K.L. Mitchell, C.D. Roberts and P.C. Tandy, Phys. Lett. **B 359** (1995) 17.
16. D. Kekez and D. Klabucar, “ $\gamma^* \gamma \rightarrow \pi^0$ transition and asymptotics of $\gamma^* \gamma$ and $\gamma^* \gamma^*$ transitions of other unflavored pseudoscalar mesons,” hep-ph/9812495; and these proceedings.
17. P.C. Tandy, these proceedings.
18. M.A. Pichowsky and T.S. Lee, Phys. Rev. **D56** (1997) 1644.
19. F.T. Hawes and M.A. Pichowsky, “Electromagnetic form-factors of light vector mesons,” nucl-th/9806025.